

Pneumatic Networks for Soft Robotics that Actuate Rapidly

Bobak Mosadegh, Panagiotis Polygerinos, Christoph Keplinger, Sophia Wennstedt, Robert F. Shepherd, Unmukt Gupta, Jongmin Shim, Katia Bertoldi, Conor J. Walsh, and George M. Whitesides*

Soft robots actuated by inflation of a pneumatic network (a “pneu-net”) of small channels in elastomeric materials are appealing for producing sophisticated motions with simple controls. Although current designs of pneu-nets achieve motion with large amplitudes, they do so relatively slowly (over seconds). This paper describes a new design for pneu-nets that reduces the amount of gas needed for inflation of the pneu-net, and thus increases its speed of actuation. A simple actuator can bend from a linear to a quasi-circular shape in 50 ms when pressurized at $\Delta P = 345$ kPa. At high rates of pressurization, the path along which the actuator bends depends on this rate. When inflated fully, the chambers of this new design experience only one-tenth the change in volume of that required for the previous design. This small change in volume requires comparably low levels of strain in the material at maximum amplitudes of actuation, and commensurately low rates of fatigue and failure. This actuator can operate over a million cycles without significant degradation of performance. This design for soft robotic actuators combines high rates of actuation with high reliability of the actuator, and opens new areas of application for them.

full range of bending (see SI). This requirement for large changes in volume limits the performance of soft actuators that use pneu-nets in three ways: i) It requires the transfer of large volumes of gas for actuation. As a result, the rate of actuation is slow. ii) It generates a change of volume of the actuator that is significant. As a result, it requires that the system be surrounded by a large volume of empty space for it to operate. iii) It imposes high strains on the material of which the pneu-net is fabricated. As a result, the operating lifespan of the pneu-net is shortened. To circumvent these limitations, we have developed a new design for a pneu-net that is better suited for high-speed, large-amplitude motion than the design described previously.^[1–7] The new actuator bends completely—from a linear rod (10 cm) into an approximate circle—at speeds greater than 1 m/s for the tip of the actuator, and in intervals as short as 50 ms.

1. Introduction

Elastomeric actuators powered pneumatically are of particular interest for soft robotics because they can be lightweight, inexpensive, easily fabricated, and able to provide non-linear motion with simple inputs.^[1–7] Pneu-nets (networks of small channels embedded in elastomeric structures that can be inflated with low pressures—approximately 50 kPa—of air) usually require a change in volume of $\sim 20\times$ their initial volume to achieve their

This silicone-based actuator also has two other features: i) it is sufficiently durable that it can sustain intermediate-frequency (4 Hz), large-amplitude motion for greater than a million repeated cycles, without failure. ii) It shows a new mode of actuation. At low rates of inflation, it bends into approximately a circle with all chambers inflating uniformly; at high rates of inflation, it curls upon itself with the chambers at its tip inflating first. To mimic the speed, if not the force, of a moving human finger, we fabricated a set of pneu-nets that played a tune on an electric piano.

Dr. B. Mosadegh, Dr. C. Keplinger, S. Wennstedt,
Dr. R. F. Shepherd, U. Gupta, Prof. G. M. Whitesides
Department of Chemistry and Chemical Biology
Harvard University
12 Oxford Street, Cambridge, MA, 02138, USA
E-mail: gwhitesides@gmwgroup.harvard.edu
Dr. B. Mosadegh, Prof. C. J. Walsh,
Prof. G. M. Whitesides
Wyss Institute for Biologically Inspired Engineering
Harvard University
60 Oxford Street, Cambridge, MA, 02138, USA
Dr. P. Polygerinos, Dr. J. Shim, Prof. K. Bertoldi, Prof. C. J. Walsh
School of Engineering and Applied Sciences
Harvard University
Cambridge, MA, 02138, USA



2. Background

Soft robots are machines fabricated from compliant materials (polymers,^[1–8] elastomers,^[1] hydrogels,^[9,10] granules^[11]); they can operate with several different modes of actuation (i.e., pneumatic,^[1,5,11–13] electrical,^[7,14–18] chemical^[12,19,20]), and their motion can be either fast (>1 Hz)^[9,12,14] or slow (<0.1 Hz).^[1,21]

Exploration of rapid motion in soft robotics is just beginning, and examples are at a level of initial demonstrations.^[1,9,12,14] For example, the “GoQBot” developed by Trimmer et al., is a worm-like robot that performs a single rapid actuation (<100 ms) to achieve a ballistic rolling motion by using the deformation of coils of shape-memory alloy (SMA).^[14] Although the body of

DOI: 10.1002/adfm.201303288

the robot is made of soft materials, the rigidity of the coils of SMA restricts the movement of the robot to a single trajectory. In contrast, pneu-nets use a non-rigid actuator (i.e., inflatable channels fabricated in an elastomeric material) that allows its trajectory of motion (i.e., the shape it bends into) to change when encountering different external forces.^[1,4,5] It is the compliance of the materials used for pneu-nets, however, that contributes to their three major weaknesses, i) slow actuation speed, ii) large change in volume, and iii) short lifespan.

High-speed actuation of a tripod robot has been accomplished using the explosion of a mixture of methane and oxygen in a pneu-net, to generate a rapid (msec) pulse of pressure, and power a jumping motion (>30 cm at 3.6 m/s).^[12] Although this explosion produced rapid motion, it is not presently adaptable to give precise control of the movement of the robot. Combustion is also not a suitable source of power for applications such as medicine. Soft robotics, therefore, need pneu-nets that actuate rapidly (>1Hz), over their full range of motion, with conventional, safe methods.

3. Results

3.1. Experimental Design

The angular speed of bending of a structure actuated by a pneu-net depends upon: i) the rate of inflation, ii) the geometry of the internal channels and exterior walls, and iii) the properties of the structure (i.e., materials used for fabrication). We use pneumatic actuation, since pressurized air has four advantages: i) it provides rapid inflation of the pneumatic structure (because air has low viscosity and can be moved rapidly); ii) it is easily controlled and measured (using regulators and sensors); iii) it is almost universally available (either from compressed gas tanks or compressors); iv) it is light in weight; iv) it can be discarded after use by venting to the atmosphere. Because it is easy to fabricate prototype pneu-nets, we tested the new geometry empirically rather than by modeling it. We did, however, clarify and visualize strains in these systems during actuation, using simulations based on finite-element models (FEMs). We fabricated all of the actuators using silicone-based elastomers, since they are commercially available, easy to work with, and able to tolerate large strains (>700%).^[22]

3.2. Design of Rapidly Actuating Pneu-Nets

We have previously described actuators based on pneu-nets.^[1,5,6] These systems have consisted, in general, of an extensible top layer and an inextensible but flexible bottom layer (Figure 1A); in this paper, we will refer to this type of structure as a “slow pneu-net” (sPN); but the abbreviation can also refer to “simple pneu-net” since the design and fabrication of these systems is slightly simpler than the ones we describe here. The extensible layer of a sPN contains chambers connected by a single channel that, when pressurized, preferentially expand the top, and stretch the inside walls, of the chambers. This change in shape results in the bending of the entire actuator (due to the difference in the compliance of the extensible and the inextensible layers). The maximum change in volume of the channels

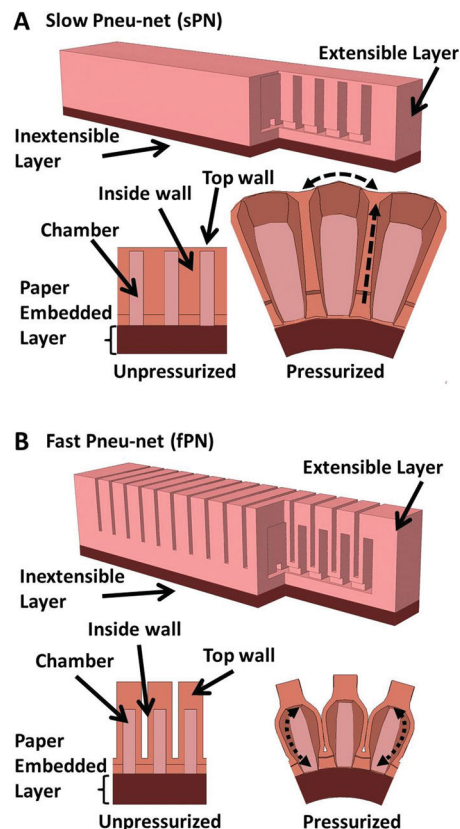


Figure 1. Design of Slow and Fast Pneu-nets. A,B) Schematic of the slow pneu-net (sPN) (A) and fast pneu-net (fPN) (B) actuators each consists of an extensible top layer, and an inextensible bottom layer reinforced with embedded paper. The top layer of the sPN actuator contains topographical features only along the inside surface of the actuator. The fPN actuator contains topographical features along the inside and outside surfaces of the actuator. Solid arrows identify regions of the actuators, and dashed arrows signify expanding regions when the actuator is pressurized.

inside the pneu-nets due to deformation of the elastomeric material defines the total amount of compressed gas that must be transported into it to achieve full bending; larger changes in volume require longer durations of pressurization to reach complete actuation.

To reduce changes in the volume required for complete actuation, and thus to increase the rate of actuation, we designed a new actuator, which we refer to as a “fast pneu-net” (fPN) (Figure 1B); the supplemental information describes its fabrication. The fPN, like the sPN, consists of an extensible top layer and inextensible, but flexible, bottom layer. In contrast to the sPN, the extensible layer of the fPN contains gaps between the inside walls of each chamber. We designed the dimensions of the chambers so that the two inside walls are thinner, and have greater surface area, than the other exterior walls. An increase in the internal pressure, therefore, preferentially expands the inside walls, and minimizes the strain that occurs on the other exterior walls. In addition, the close proximity of two neighboring chambers causes the expanding inside walls to push against each other, and results in a preferential elongation of the extensible layer with only small changes (<1%) in the height of this layer.

3.3. fPNs of Different Dimensions

To investigate the impact that different dimensions have on the bending of the fPN, we characterized the pressure required to bend it for different numbers of chambers, heights of chambers, and wall thicknesses of the chambers (Figure S2). Empirically we determined that more chambers for a given length and thinner inside walls enabled greater bending at lower pressures (Figure S2). The extent to which these trends can be exploited, however, is limited both by the properties of the materials, and by the fabrication of the pneu-nets. The resolution of the 3D printer ($\sim 300\ \mu\text{m}$ for the 3D printers used in this work), used to make the molds determines the number of chambers and thickness of the walls that can be fabricated using this mold. The effect of increasing the height of a chamber, for a given width, appears to plateau, and therefore even taller chambers would only increase the actuator size, weight, and the amount of elastomer used without increasing the performance of the actuator (Figure S2A). Although these trends suggest a guideline for designing fPNs, further work—both experimental and computational—will improve the performance of this class of actuators by exploring a larger volume of parameter space than that tested in this work.^[23]

3.4. Mass Transport Analysis of sPN and fPN

To quantify the amount of fluid (normally air, but occasionally water during characterization) transported during actuation, we measured pressure–volume (PV) hysteresis curves for a test beam containing either a sPN or a fPN, with both submerged in water to counteract the force of gravity. We correlated these measurements with the extent of bending using continuous video recordings (Figure 2A,B). A syringe pump (Harvard Apparatus PHD 2000) transferred water (an incompressible fluid) into the actuator at a rate of inflation and deflation ($0.07614\ \text{mL/s}$) that was sufficiently slow to achieve quasi-static conditions. The incompressibility of the fluid allowed us to equate the volume decrease/increase of fluid in the syringe to that of the increase/decrease in the volume of the channels in the pneu-net. A pressure transducer, connected directly between the actuator and the syringe pump, monitored the pressure inside the system continuously (Figure S3). Each PV hysteresis curve displays the pressure and volume levels necessary to achieve full bending (that is, sufficient bending that the two ends of the actuator touch) and deflation back to the initial state.

Six parameters describing the performance of the actuators can be extracted from the PV hysteresis plots generated using this procedure: i) the pressure of fluid required for full actuation; ii) the volume of fluid required for full actuation; iii) the input energy required for full bending of the actuator; iv) the energy that can be recovered during depressurization; v) the energy dissipated during one cycle of actuation; and vi) the shape (linearity or type of non-linearity) of the PV curve. The maximum values for the x- and y-axis signify the pressure and volume required for full bending of the actuator. The area below the inflation curve signifies the input energy of the actuator. The area below the deflation curve signifies the energy

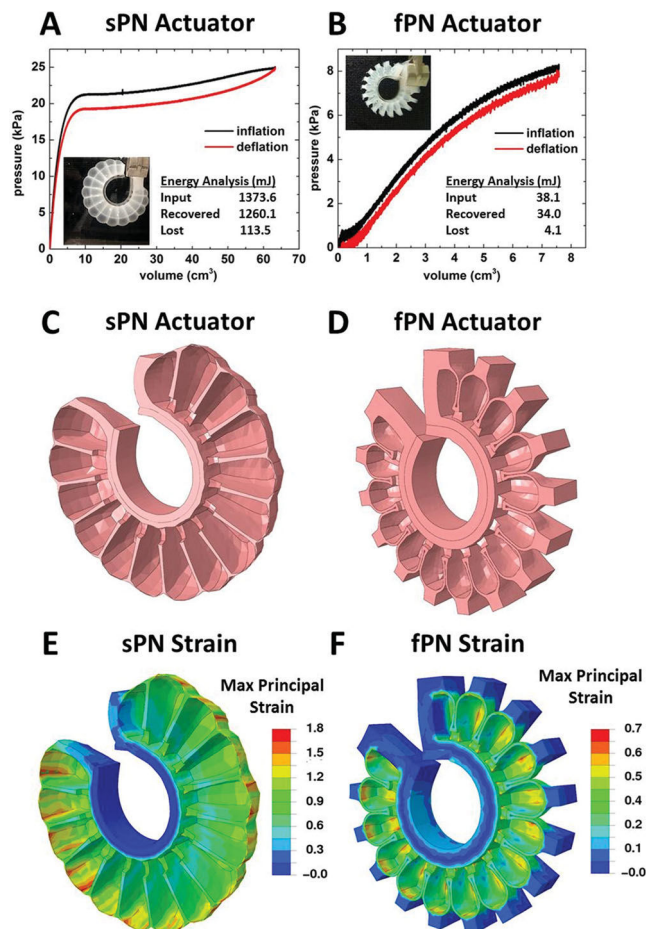


Figure 2. Comparison of fPN and sPN actuators. A,B) Pressure-volume hysteresis curves for actuators undergoing quasistatic hydraulic inflation/deflation. The areas under the inflation and deflation curves signify the amount of energy added to and recovered from the actuator. Lost energy is the difference between the input and recovered energy. Inset images show actuators at the maximum inflation pressure. C–F) Simulated bending, generated by a finite-element model, of the bending of the sPN (C,E) and fPN (D,F) actuators and the levels of the maximum principal strain (i.e., 1D dimensionless units) experienced by the actuator when fully pressurized.

recovered from the actuator. The dissipated energy equals the difference between the input and recovered energies.

To compare the sPN and fPN design, we tested actuators made from Ecoflex 30 (for the extensible layer) and Sylgard 184 PDMS (for the inextensible layer). When using Ecoflex 30/PDMS as the elastomer, the results show the sPN requires $\sim 3\times$ higher pressure, $\sim 8\times$ higher volume, $\sim 35\times$ more energy to bend fully than the fPN (Figure 2AB). In addition, during one actuation cycle, the sPN dissipated nearly $30\times$ more energy than the fPN.

The fact that the fPN undergoes smaller change in volume during inflation is critical for potential applications in space-limited settings (perhaps in procedures such as minimally invasive surgery, or movement through a pipe). The sPN requires outward expansion of its extensible layer to bend, and any restrictions on the space available for its expansion could

prevent proper function. The expansion of the extensible layer for the fPN, however, occurs largely within the space between each of its chambers, and thus allows it to move in tighter spaces.

Control of the movement of the actuator is another important parameter characterizing performance. The sPN follows a non-linear relationship between pressure and volume, in that the volume increases but pressure is relatively stable after a threshold pressure (Figure 2A). This non-linearity of the PV curve would make it difficult or impossible to measure the degree of bending of the sPN by monitoring its pressure. The fPN, however, has a nearly linear PV curve; this quasi-linearity should allow predicting movement by monitoring pressure (Figure 2B). The fPN therefore has the advantage of providing a complex non-linear output (i.e., a bending motion) with a simple near-linear input (i.e., pressure).

3.5. fPNs Fabricated with Different Elastomers

We measured PV hysteresis curves for a fPN actuator fabricated with a stiffer elastomer (Elastosil M4601, Young's modulus of ~ 7 MPa, Shore A hardness 28) for the extensible layer. In comparison to Ecoflex 30 (Young's modulus ~ 0.1 MPa, Shore A hardness 00–30), the actuator fabricated with the stiffer elastomer required nearly 8 \times more pressure, but required $\sim 1.5\times$ less change in volume to bend fully (Figure 3). The additional volume required by the dPN made of a softer elastomer is a consequence of the outward expansion of its exterior walls. These results suggest that actuators fabricated from softer elastomers exert less force, and bend more slowly for a given rate of inflation than the same actuator made of a stiffer elastomer since additional volume must be transferred to achieve the same degree of bending.

3.6. Fatigue Testing of fPNs

An important metric for the performance of elastomeric actuators is the life-span of the device in use; the life-span is limited by fatigue in the material and failure in the adhesive interface.^[24] We measured the number of full actuation cycles (each cycle consisting of nearly full bending and relaxing) that each type of actuator would withstand before bursting. The sPN (actuated at 0.33 Hz) failed, on average, after ~ 126 cycles ($n = 11$ sPN with a standard deviation of 274 cycles; Movie S1) and at most after 990 cycles. The large deviation for the failure of the sPN was due primarily to the presence of bubbles (introduced in the elastomer making up the top wall of the extensible layer during fabrication) that weaken the wall, concentrate stress, and lead to the rupture of the extensible layer. Fabricating thicker top walls of the sPN will reduce failure due to bubbles, but increase failure by delamination, since higher pressures are required for the actuator to bend fully.

The fPN avoids both modes of failure (interfacial failure and rupture of the extensible layer) by significantly reducing: i) the pressure required for full actuation, ii) the maximum strain in the top wall of the extensible layer required for bending, and iii) bubbles present in the expanding regions of the extensible

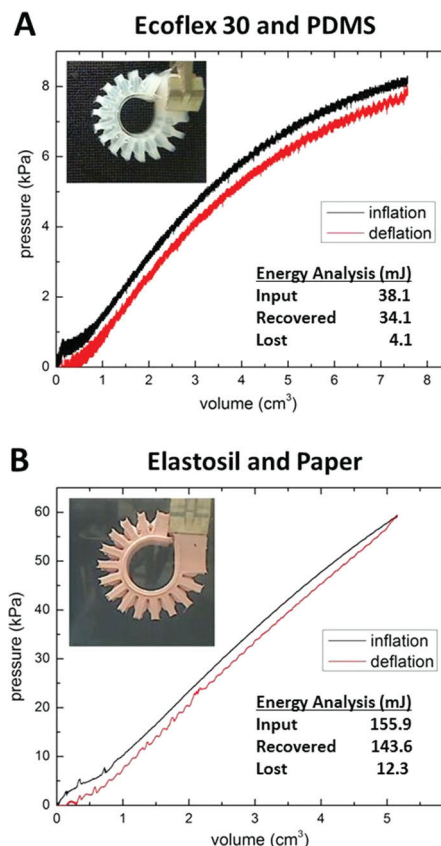


Figure 3. Effect of Elastomer Stiffness. A,B) Pressure–volume hysteresis curves for fPN actuators fabricated with an extensible layer made from Ecoflex 30 and an inextensible layer made from PDMS (A) and an extensible layer made from Elastosil M4601 and inextensible layer made from a composite of Elastosil M4601 and paper fabric (B).

layer. The fPN thus achieves a life span that is longer than we have been able to measure; the fPN did not fail after cyclic actuation at 2 Hz for 10^4 , 2×10^5 , and 10^6 cycles of complete actuation.

We assessed fatigue of the material by measuring PV hysteresis curves for three separate fPNs, before and after subjecting them to cyclic testing (Figure 4). The PV curves do not change substantially over the 10^6 cycles, suggesting that the performance was maintained. The slight decrease in slope, however, suggests that the actuator requires less pressure, but more volume, to bend fully; thus, after many cycles of actuation, the material extends slightly more easily than before the cyclic testing, possibly due to strain of the polymer chains in the elastomer.

3.7. Analysis of Strain and Force of the sPN and fPN

To estimate the local strain experienced by both a sPN and fPN, we developed a finite- element analysis using Abaqus 6.11-Simulia (Dassault Systems). For the FEM, the most critical aspect is properly modeling the non-linear elastomeric behavior of the silicone materials used (Elastosil M4601). We measured

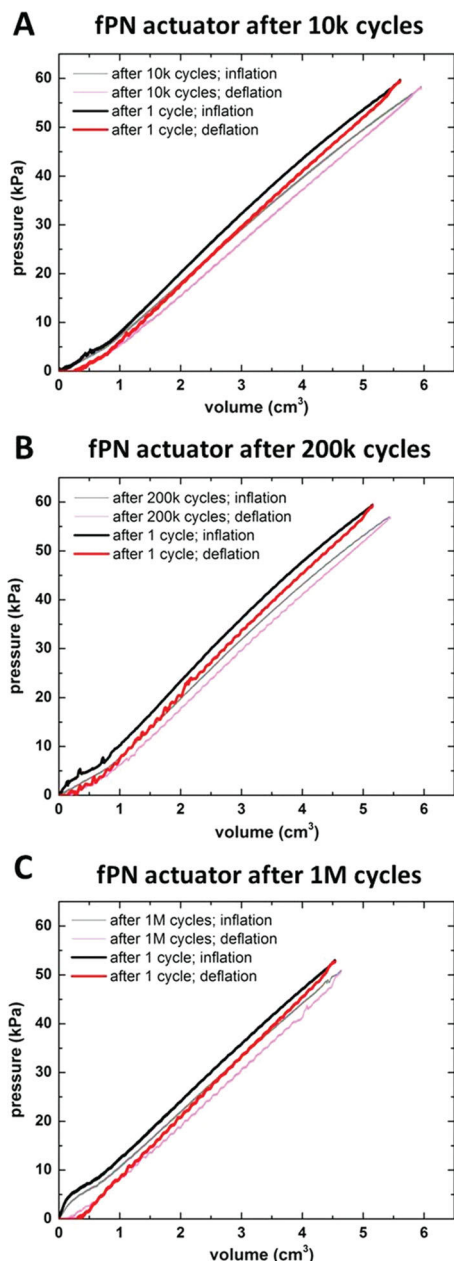


Figure 4. Fatigue test of fPN actuators. A–C) Pressure-volume hysteresis curves for fPN actuators before and after repeated pneumatic actuation. fPN actuators are made of Elastosil M4601 and paper and are hydraulically actuated to generate the PV curves.

stress-strain curves using pieces of cured Elastosil M4601, and fit the compression and tensile data to the Yeoh hyperelastic material model in Matlab (Figure S4). The FEM results show the fPN experiences significantly less ($\sim 2.5\times$) strain (maximum principal or non-deformational) than the sPN for equivalent amplitude of bending (Figure 2C–F).

To validate our FEM, we characterized the pressure required to bend a sPN and a fPN with the same number of chambers (15), same height of chambers (10.5 mm), and same wall thickness (1 mm) (Figure S5). We tracked the trajectory of the free

end of the actuator using images taken from a camera, and plotted them using a graph that allowed comparison of experimentally observed positions, and positions predicted by the FEM (Figure S5E, F). The fPN reached its full range of motion (360° bending) at 72 kPa (Figure S7D); at this pressure, the sPN deflected only 41° (Figure S5C).

We also investigated the force these actuators exert for a given pressure to validate the accuracy of the FEM (Figure S6). Using a transducer (Nano17, 6 axis F/T sensor, ATI industries), we measured the force exerted by the tip of the actuator when the opposite end was fixed in place. As with the actuator trajectories, the forces predicted by the FEM for the sPN and fPN were of good agreement with experimental measurements; this agreement suggests the simulated values of strain are accurate. A fPN applied a force of ~ 1.4 N for an actuation pressure of 72 kPa (the pressure that provided full range of bending for the fPN). At the same pressure, a sPN having analogous dimensions applied a force of ~ 1 N, (i.e., 40% less than that of the fPN). By increasing the applied pressure (until the actuators rupture), both the sPN and fPN can apply additional force. Changing the stiffness of the elastomer can tune the range of forces exerted by both actuators (silicone and polyurethane elastomers with a large range of material properties are commercially available).

3.8. Rapid Actuation of the sPN and fPN

To compare how rapidly the sPN and fPN bend, we actuated each with a miniature compressor (BTC-IIS, Parker, Hollis, NH), which delivers compressed air at pressures up to 193 kPa, at a maximum flow rate of ~ 11 L/min (Movie S2 and S3). Using this compressor, on average, the sPN bends fully in 3.3 seconds (standard deviation of 0.54 s for $N = 7$ actuations) and the fPN bends fully in 130 ms (standard deviation of 8 ms for $N = 7$ actuations).

To determine the maximum frequency the fPN could bend, we used a computer-controlled solenoid valve to pulse pressurized gas for short durations, and then vented the system to equilibrate with atmospheric pressure (Figure 5A, Movie S4); the head pressure (that is, the pressure set by the regulator) was adjusted to achieve full bending of the fPN. The highest frequency of full bending and relaxing achieved by the fPN, using a 50% duty cycle (equal durations of pressurizing and venting periods), was 2 Hz using 76 kPa head pressure (Figure 5B). Higher frequencies did not allow the actuator to return to its original position. We employed a duty cycle with a shorter pressurization period (50 ms using 448 kPa head pressure) and a longer venting period (200 ms) to achieve an overall higher frequency (4 Hz) of actuation (Figure 5C, Movie S5).

Figure 5D shows snapshots taken from a movie using a high-speed camera (1000 fps) of the fPN actuator (Movie S6, S7). The fPN showed an interesting and potentially very useful bi-modal behavior; the change between modes occurs above ~ 200 kPa head pressure. For slower rates of actuation, the chambers of the fPN inflate relatively evenly, and the actuator bends along a roughly circular trajectory. Above the threshold rate, however, the tip of the actuator bends preferentially, and causes the actuator to curl on itself.

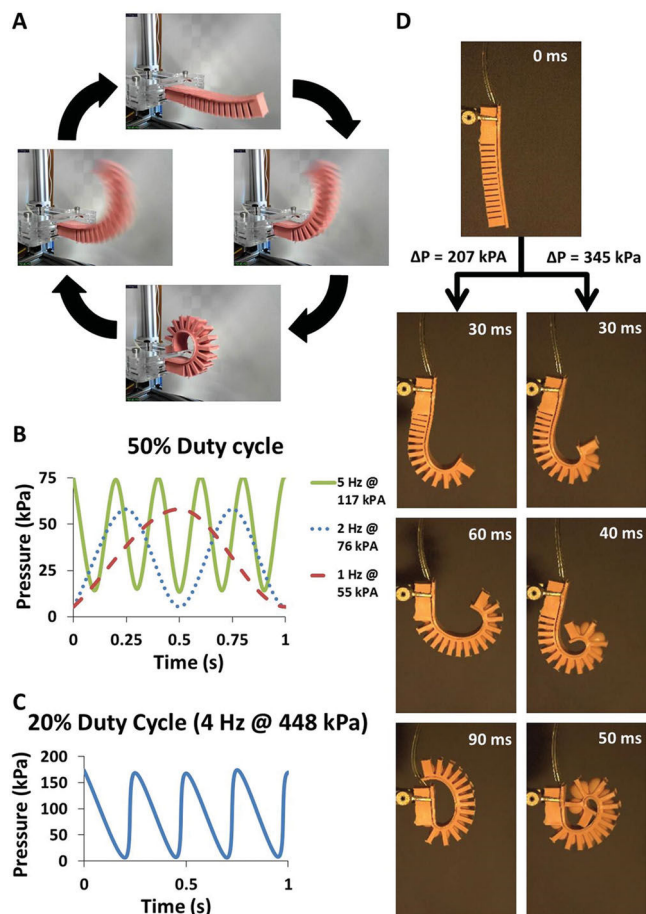


Figure 5. High-Speed Actuation. A) Images of different positions of the fPN actuator during a full actuation cycle. B) Profile of the internal pressure of the actuator for three frequencies with 50% duty cycle at pressures that cause full bending of the actuator. C) Profile of the internal pressure for 20% duty cycle (50 ms pressurization, 200 ms venting) at 413 kPa that yields an actuation frequency of 4 Hz. D) Time-lapse images from high-speed videos of the fPN actuator when actuated with two different pressurization rates. The actuator bends preferentially at its tip for the higher rate and more uniformly for the lower rate.

3.9. Pneu-nets Playing a Keyboard

For maximum utility, soft actuators must have the ability to perform useful tasks rapidly. To provide an example using fPNs, we set four to play an electronic keyboard in a way that mimics (at least distantly) human fingers (**Figure 6A**). The actuators require sufficient speed to maintain a desired tempo, and sufficient force (0.650 N) to depress the keys. The portion of the fPN that contacts the key weighs ~4.5 g and its gravitational weight can therefore only produce a maximum of 0.045 N of force. The remaining force (0.605 N) required to depress a key must be that of the actuator itself (i.e., the internal pressure acting on the actively bending region of the actuator, and the kinetic energy resulting in a transfer of momentum from that bending region of the actuator). We used a solenoid valve to control whether the fPN was pressurized with compressed air (103 kPa was the maximum pressure of our control system) or vented

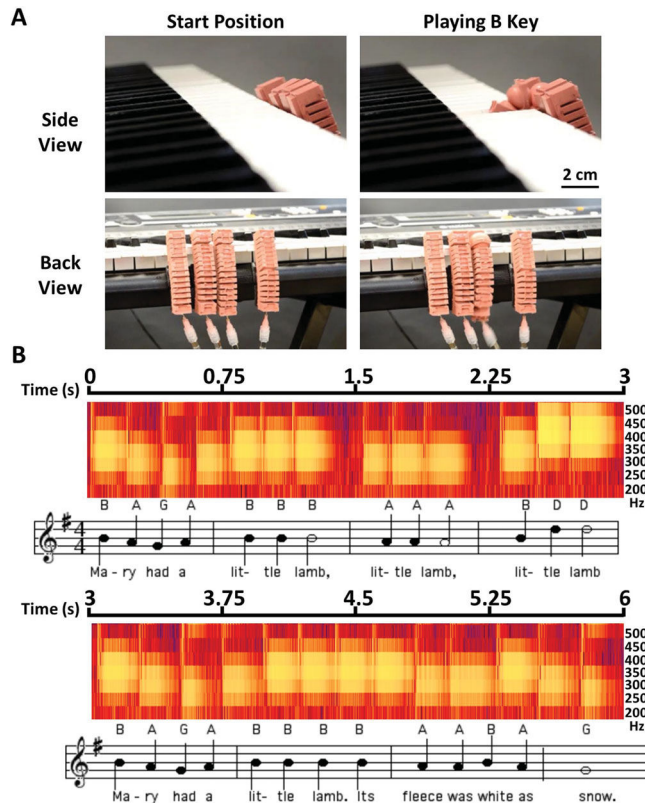


Figure 6. Independent Output Control. A) Images from two views of four fPN actuators playing a tune on a digital keyboard. Video is available in the on-line supplemental information. Each fPN was actuated for 75 ms at 103 kPa (except for repeated notes, which were actuated for 50 ms) and vented for 150 ms. B) Spectrum analysis of the audio file for frequencies between 200 and 500 Hz.

to the atmosphere; tubing (21 cm long and 3.5 mm in diameter); a needle (16 gauge) connected the fPN directly to the solenoid valves. The actuator hit the key ~100 ms after opening the valve; to do so, its tip traveled a distance of ~2.6 cm, yielding a momentum of $\sim 1.3 \times 10^{-7}$ Ns and a force of ~0.005 N. The majority (~0.6 N) of the force used to depress a key, therefore, results from the pressurization of the fPN.

To demonstrate the precision and speed of the fPN actuators, we used four fPNs to play “Mary Had a Little Lamb” on the keyboard (**Figure 6B**; Movie S8). We fixed these actuators on the side of the keyboard using Velcro, and actuated them with pressurized air using computer-controlled solenoid valves. Playing a note required a period of pressurization of 75 ms (with a head pressure of 103 kPa), and a venting period of 150 ms.

Notes played in succession (the same actuator pressurized twice in a row) required a 50 ms pressurization time, so the actuator would release the key more quickly (alternatively, a longer venting time could have been used, but would have required a slower tempo; **Figure 6A**). **Figure 6B** shows the spectrum analysis of the audio file. The notes played by the fPN match those of the song, and are clearly resolved. This resolution provides one demonstration of the precision of these actuators. The entire two staves play within 6 s, and three notes play in as little as 0.4 s. To play songs with shorter intervals between

notes, we could increase the flow rate of air by using higher pressures (>103 kPa), larger diameter tubing (>3.5 mm), faster mechanisms of venting (e.g., vacuum-driven venting, integrated venting holes directly in the fPNs), and more optimized positioning of the fPNs.

4. Conclusions

The performance of a pneu-net can be classified into at least five parameters, i) speed achieved for a given rate of inflation, ii) force exerted for a given pressure, iii) change in volume required for a given degree of bending, iv) number of actuation cycles before failing, and v) correlation between the pressure in the pneu-net and its degree of bending without a load. The fPN improves on all these parameters and therefore is better suited for actuating soft robots than the sPN.

Specifically, the improved speed (25 ×) and force (1.4 ×) of the fPN relative to the sPN will be useful for creating soft robots that move more quickly, and can exert higher forces, than could be achievable with the sPN. Alternatively, one could actuate fPNs with a smaller compressor and obtain performance similar to that generated using a larger compressor and sPNs; the advantage of the system based on the fPN being a reduction in the overall size and power-consumption of the robot (an option particularly useful for untethered applications).

The reduced change in volume (8× smaller than the sPN) minimizes fatiguing of the material, and thus improves the durability of the fPN to such a level that the actuator does not fail within a million cycles of full bending (Figure 4). This high durability could allow its use in long-term applications, and when high margins of safety are required for high-consequence uses (such as in medical procedures). The large window of operating temperatures (−20 to 300 °C) for silicones allow the use of these actuators in a variety of environments.^[25] Furthermore, since the fPN expands into the space between the chambers, the actuator assumes a smaller volume upon inflation, and thus has the potential to enter smaller spaces; this attribute is beneficial for some applications in search-and-rescue and minimally invasive surgery.

In addition to improving the performance (i.e., speed and force) of pneu-nets, we have demonstrated that the rate of actuation (as opposed to the geometry of the actuator) could determine the motion of a pneu-net (Figure 5D). The bi-modal bending behavior that occurs at high speeds may provide interesting opportunities for control schemes, by allowing at least two different types of motion from a single design, simply by changing the rate of pressurization. Further exploration of this rate-dependent behavior may prove fruitful in developing sophisticated soft actuators that can perform tasks that are more useful than playing a keyboard (Figure 6).

There are two limitations of the specific fPN design described in this work: i) the fPNs bend slightly when gravity acts on the actuator with its bottom layer facing downward, since the chambers connect only at their base, and thus act like a loose hinge (Figure S5B). Adding material between the chambers or using stiffer materials for the top or bottom layer could prevent this initial bending angle (at the cost of requiring more pressure to actuate the fPN). ii) The chambers of the fPN do not

expand uniformly when pressurized above their full bending amplitude due to snap-through instability of the elastomeric material.^[26] Although this non-linear behavior may have potential advantages, it also prevents the fPN from exerting forces along its length uniformly. To prevent this behavior, the expansion of the inside walls of the chambers need to be restrained by an inextensible material.^[3]

5. Experimental Section

Details of fabrication and design for the fPNs are available in the supplementary information. In brief, we used 3D printing to make molds, and soft lithography using those molds to fabricate fPNs. For pneumatic actuation, we pressurized the fPNs with gas supplied from house nitrogen, and vented the chambers on deflation to the atmosphere; computer-controlled solenoid valves regulated actuation of the fPNs. For hydraulic actuation, we used a digital syringe pump that provides a constant flow rate for both inflation and deflation of the fPNs. We used both a web-cam and a high-speed camera to observe the movement of the fPNs during actuation.

Supporting Information

Supporting Information is available from the Wiley Online Library or from the author.

Acknowledgements

PV hysteresis curves for comparing the performance of different elastomers and fatigue testing of the actuators and funding for Christoph Keplinger was supported by the Department of Energy (DE-FG02-00ER45852). DARPA (award number W911NF-11-1-0094) supported Robert Shepherd, Sophia Wennstedt, and the development of the actuators and their application to playing the keyboard and rate-dependent bending. We thank the Wyss Institute for Biologically Inspired Engineering for providing support to Bobak Mosadegh and Panagiotis Polygerinos and MRSEC (grant DMR-0820484) for providing funding to Jongmin Shim.

Received: September 23, 2013

Revised: October 26, 2013

Published online:

- [1] F. Ilievski, A. D. Mazzeo, R. F. Shepherd, X. Chen, G. M. Whitesides, *Angew. Chem. Int. Ed.* **2011**, *50*, 1890.
- [2] R. V. Martinez, J. L. Branch, C. R. Fish, L. Jin, R. F. Shepherd, R. M. Nunes, Z. Suo, G. M. Whitesides, *Adv. Mater.* **2013**, *25*, 205.
- [3] R. V. Martinez, C. R. Fish, X. Chen, G. M. Whitesides, *Adv. Funct. Mat.* **2012**, *22*, 1376.
- [4] S. A. Morin, R. F. Shepherd, S. W. Kwok, A. A. Stokes, A. Nemiroski, G. M. Whitesides, *Science* **2012**, *337*, 828.
- [5] R. F. Shepherd, F. Ilievski, W. Choi, S. A. Morin, A. A. Stokes, A. D. Mazzeo, X. Chen, M. Wang, G. M. Whitesides, *Proc. Natl. Acad. Sci. USA* **2011**, *108*, 20400.
- [6] S. Wakimoto, K. Suzumori, K. Ogura, *Adv. Rob.* **2011**, *25*, 1311.
- [7] A. A. Stokes, R. F. Shepherd, S. A. Morin, F. Ilievski, G. M. Whitesides, *Soft Robotics* **2013**, *1*, 70.
- [8] L. W. Shi, S. X. Guo, M. X. Li, S. L. Mao, N. Xiao, B. F. Gao, Z. B. Song, K. Asaka, *Sensors* **2012**, *12*, 16732.

- [9] H. Lee, C. G. Xia, N. X. Fang, *Soft Matter* **2010**, *6*, 4342.
- [10] M. Otake, Y. Kagami, M. Inaba, H. Inoue, *Rob. Auto. Sys.* **2002**, *40*, 185.
- [11] E. Brown, N. Rodenberg, J. Amend, A. Mozeika, E. Steltz, M. R. Zakin, H. Lipson, H. M. Jaeger, *Proc. Natl. Acad. Sci. USA* **2010**, *107*, 18809.
- [12] R. F. Shepherd, A. A. Stokes, J. Freake, J. Barber, P. W. Snyder, A. D. Mazzeo, L. Cademartiri, S. A. Morin, G. M. Whitesides, *Angew. Chem. Int. Ed.* **2013**, *52*, 2892.
- [13] C. P. Chou, B. Hannaford, *IEEE Trans. Robot. Autom.* **1996**, *12*, 90.
- [14] H. T. Lin, G. G. Leisk, B. Trimmer, *Bioinspir. Biomim.* **2011**, *6*, 026007.
- [15] F. Carpi, S. Bauer, D. De Rossi, *Science* **2010**, *330*, 1759.
- [16] G. Kofod, W. Wirges, M. Paajanen, S. Bauer, *Appl. Phys. Lett.* **2007**, *90*, 081916.
- [17] C. Keplinger, M. Kaltenbrunner, N. Arnold, S. Bauer, *Proc. Natl. Acad. Sci. USA* **2010**, *107*, 4505.
- [18] M. Shahinpoor, Y. Bar-Cohen, J. O. Simpson, J. Smith, *Smart Mat. Struct.* **1998**, *7*, R15.
- [19] C. D. Onal, D. Rus, in *Proceedings of the 2012 International Conference on Biomedical Robotics and Biomechanics*, **2012**.
- [20] E. Palleau, D. Morales, M. D. Dickey, O. D. Velev, *Nat. Commun.* **2013**, *4*, 2257.
- [21] J. D. W. Madden, N. A. Vandesteeg, P. A. Anquetil, P. G. A. Madden, A. Takshi, R. Z. Pytel, S. R. Lafontaine, P. A. Wieringa, I. W. Hunter, *IEEE J. Oceanic Eng.* **2004**, *29*, 706.
- [22] Wacker Silicone Rubbers, RTV-2, <http://www.wacker.com/cms/en/products-markets/products/product.jsp?product=9125&country=US&language=en>, (accessed: October, **2013**)
- [23] N. Cheney, R. MacCurdy, J. Clune, H. Lipson, in *Proceedings of the Genetic and Evolutionary Computation Conference*, **2013**.
- [24] T. Zarrin-Ghalami, A. Fatemi, *Fatigue Fract. Eng. Mater. Struct.* **2013**, *36*, 270.
- [25] Characteristics Properties of Silicone Rubber Compounds, http://www.silicone.jp/e/catalog/pdf/rubber_e.pdf, (accessed: October, **2013**)
- [26] T. Li, C. Keplinger, R. Baumgartner, S. Bauer, W. Yang, Z. Suo, *J. Mech. Phys. Solids* **2013**, *61*, 611.

ADVANCED FUNCTIONAL MATERIALS

Supporting Information

for *Adv. Funct. Mater.*, DOI: 10.1002/adfm.201303288

Pneumatic Networks for Soft Robotics that Actuate Rapidly

*Bobak Mosadegh, Panagiotis Polygerinos, Christoph
Keplinger, Sophia Wennstedt, Robert F. Shepherd, Unmukt
Gupta, Jongmin Shim, Katia Bertoldi, Conor J. Walsh,
and George M. Whitesides**

Supporting Information

for *Adv. Funct. Mater.*, DOI: 10.1002/adfm.201303288

Pneumatic Networks for Soft Robotics that Actuate Rapidly

*Bobak Mosadegh, Panagiotis Polygerinos, Christoph Keplinger, Sophia Wennstedt, Robert F. Shepherd, Unmukt Gupta, Jongmin Shim, Katia Bertoldi, Conor J. Walsh, and George M. Whitesides**

Fabrication of fPN Actuator

The fPN actuators were made similarly to sPN actuators, as described previously¹⁻³. First, molds were made in acrylonitrile butadiene styrene (ABS) using a three-dimensional (3D) printer (Dimension 3D; Stratasys, Inc.) based on a computer-aided-design (CAD) drawing (Solidworks Corp, Waltham, MA). The fPN actuator required three molds: an interior and exterior mold for the top extensible layer and a third mold for the bottom inextensible layer (Fig. S1). The interior mold consisted of chambers connected by a single channel, so that all chambers inflate simultaneously. The connecting channel had a smaller height (1 mm) than the chambers (10.5 mm); this difference caused the chambers to expand preferentially when pressurized. The features of the exterior mold consisted of straight parallel plates that fit in between each chamber of the interior mold. The plates separate the elastomeric material between each chamber such that no two chambers shared an inside wall.

We fabricated the bottom layer by pouring elastomer in a flat mold that contained a piece of paper, which served as the inextensible material. The top layer was placed inside the bottom layer before curing so that the elastomer was cured in place. Alternatively, the paper can be bonded after curing of the bottom layer using a silicone adhesive such as Elastosil E951 (Wacker Chemical Corp., Adrian, Michigan) (Fig. S1C). We used two types of elastomers, Ecoflex 30 (Smooth-On Inc., Easton, PA) and Elastosil M4601 (Wacker Chemical

Corp., Adrian, Michigan), which are both two-component silicone rubbers that polymerize at room temperature. Ecoflex 30 is extremely soft (shore value of 00-30) and Elastosil M4601 is relatively stiff (shore A30). We made inlet holes using a 2-mm biopsy punch at one end of the actuator. Using tubing of a slightly larger diameter (1/32" inner, 3/32" outer) than the inlet provided an adequate seal. Actuators were pressurized by compressed air or nitrogen supplied by gas tanks. Hydraulic actuation was also performed using water supplied by a syringe pump.

Silicone is permeable to gases and water and therefore actuators made of this material require continuous pressurization to maintain a fixed position. Use of non-volatile liquids, such as ionic liquids, could be used for long-term uses of these actuators⁴.

Characterization of fPN actuator

We tested the various designs of the fPN actuators by measuring the pressure required to bend them fully (Fig. S2). We used a pressure regulator (Type 700, Control Air Inc., Amherst, NH) to control the delivery of pressurized gas to the actuator. We considered an actuator fully bent when both ends of the actuator were in contact. A pressure gauge (MGA-30-A-9V-R, SSI technology Inc., Janesville, WI), directly connected to the actuator by tygon tubing (1/32" inner, 3/32" outer), displayed the pressure. We captured images of the actuators in their bent positions using a Nikon D5100 camera.

Pressure-Volume (PV) curves

We generated PV hysteresis curves by hydraulic inflation and deflation of the actuators in a 10-gallon fish tank. We fixed a syringe pump (Harvard Apparatus, PHD 2000)

and pressure sensor (Transducers Direct, TDH30) in an orientation parallel to the surface of the water (Fig. S3). We clamped the actuator fully submerged in the water in a vertical position and placed a grid (2.5 x 2.5 mm) behind it for reference. We filled the actuators with water by submerging them in water and applying a vacuum several times until bubbles would no longer emerge (squeezing the actuators under water also enabled effective removal of air).

Within each test, we switched from inflation to deflation when the actuator had achieved full bending, which we considered to be when the free end of the actuator touched its fixed end, and thus created a full circle. Once the actuator had completed one full cycle and the pressure returned to zero, we inflated it again to assure reproducibility. We repeated this procedure for at least three cycles.

A sPN has an internal volume of ~3.2 ml, measured by the differential weight before and after filling the actuator with water. The sPN requires ~63 ml of water to inflate to its full range of bending (see Fig. 2A). Therefore the volume of the sPN expands by ~20 times its initial volume. The fPN has the same internal volume but only requires ~7.5 ml of water to achieve its full range of bending (see Fig. 2B). The fPN, therefore, only expands by ~ 4 times its initial volume.

Finite Element Model of the sPN/fPN actuator

To investigate the distribution of strains during actuation in the sPN and fPN actuators we built 3D models and used the commercial finite element (FE) software Abaqus FEA for the analysis, employing the the Abaqus/Standard solver. The geometry of the actuator was imported into Abaqus CAE as a stl file and meshed using solid quadratic tetrahedral elements (Abaqus element type C3D10H) for all the elastomeric components of the actuators and shell

elements (Abaqus element type STRI65) for the inextensible layer of paper. The accuracy of each mesh was ascertained through a mesh refinement study, resulting in a model with 19,826 solid and 738 shell elements for the case of the sPN actuator and 26,593 solid and 845 shell elements for the case of the fPN actuator.

To capture the response of the elastomer used to fabricate the actuators (Elastosil), we modeled the material as a hyper-elastic solid and computed the stresses and elastic energies using the nearly-incompressible Yeoh model⁵, whose strain energy density is given by

$$U = \sum_{i=1}^N C_{i0} (\bar{I}_1 - 3)^i + \sum_{i=1}^N \frac{1}{D_i} (J - 1)^{2i} \quad (1)$$

where $\bar{I}_1 = tr[dev(\mathbf{FF}^T)]$, $J = \det(\mathbf{F})$, and \mathbf{F} is the deformation gradient and C_{i0} and D_i are the materials parameters. Here, we used $N=3$ and $C_{10}=0.11$, $C_{20}=0.02$, $C_{30}=0$, $D_1=D_2=D_3=0$. Moreover, the response of the inextensible layers was captured using a linear elastic model with a Young's Modulus of 6.5 GPa and a Poisson's ratio of 0.2.

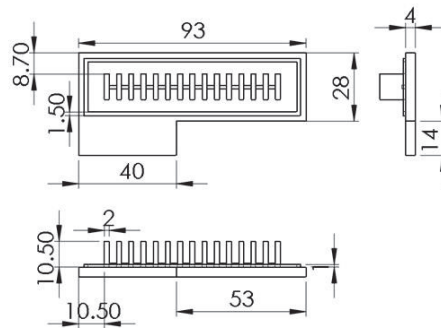
Thereafter, static simulations were performed applying pressure on all internal faces of the cavities and assuming zero displacements at the top and bottom face of the proximal pneu-net chamber to simulate the experimental boundary conditions. Gravitational forces were taken into account in the simulations.

Characterizing the Rapid Actuation of fPNs

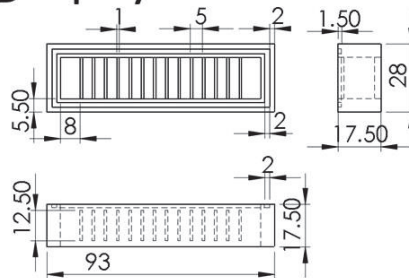
To demonstrate the rapid actuation of the fPN, we incorporated multiple sensing modalities (pressure/flow sensors and high definition cameras) to obtain information on the performance of the fPNs. Using this system, we mounted one end of the fPN on a rigid fixture so it could perform its full range of bending without any obstruction by the fixture. A

source of regulated (P31-pressure regulator, Parker Hannifin Corp.) pressurized air was connected to the actuator. Two solenoid valves (X-Valve, Parker Hannifin Corp.) supplied and vented the air. A graphical user interface (LabView 2012, National Instruments) controlled the pressure regulator and monitored the flow rate (AWM5000, Honeywell) and pressure (ASDX Series, Honeywell) of air transferred to and from the actuator. A data acquisition card (NI USB-6211, National Instruments) interfaced the hardware and software and regulated the timing of the valves through electronic relays (SRD-05VDC-SL-C Power Relay, Songle Relay Co.).

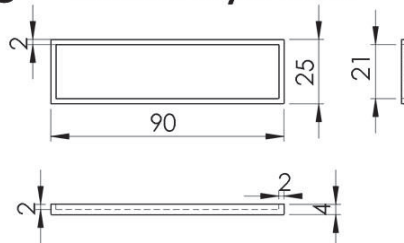
A Top Layer- Interior Mold



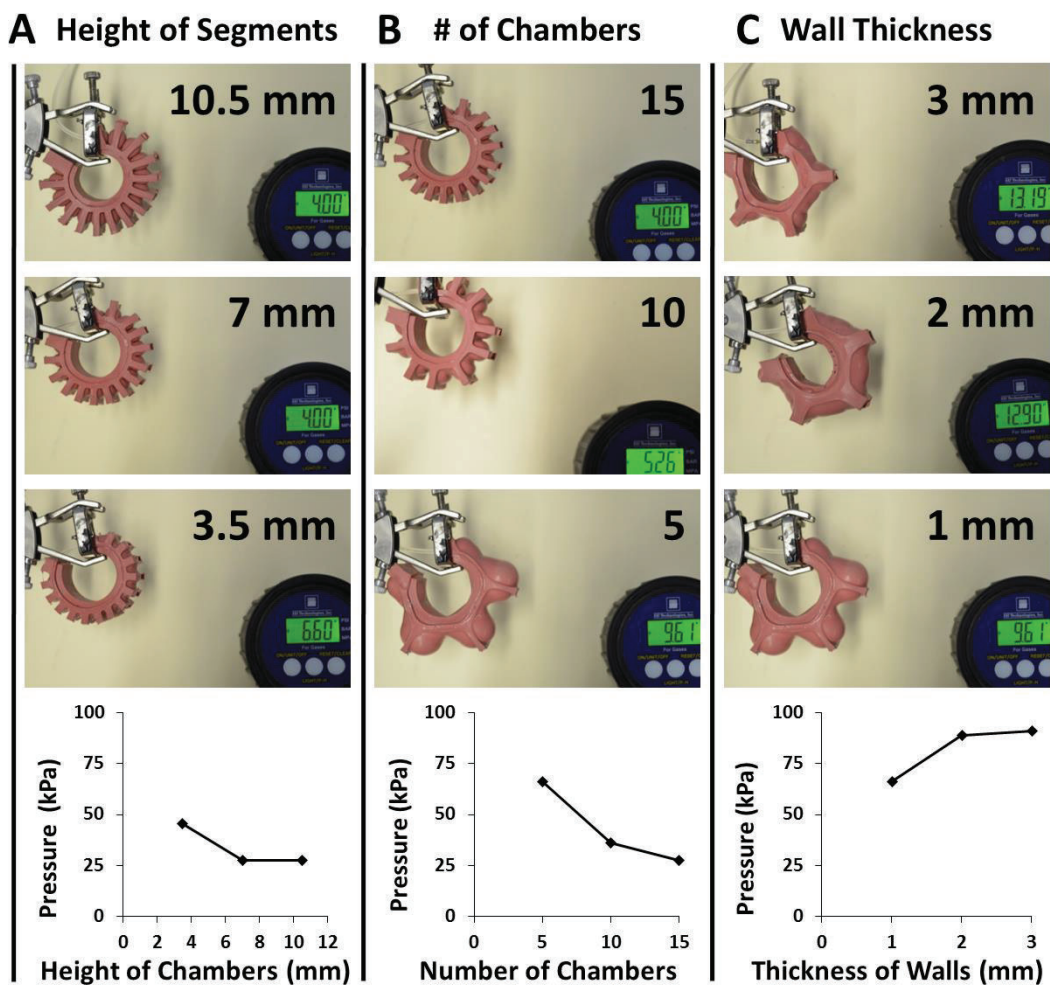
B Top Layer- Exterior Mold



C Bottom Layer Mold



Supplemental Figure S1. Molds for Fabricating a fPN Actuator. A) Dimensions (mm) for the interior mold for the top layer of the fPN actuator. Shown are 2D sketches of the top, side, and back views of the molds. B) Dimensions for the exterior mold for the top layer of the fPN actuator. Shown are 2D sketches of the bottom, side, and back views. C) Dimensions for the mold for the bottom layer of the fPN actuator. Shown are 2D sketches of the top, side, and back views.



Supplemental Figure S2. fPNs of Different Geometries. A-C) Pressure each actuator

required to bend fully (gauges show pressure in psi). A) Varied channel height with a constant number of chambers (15) and thickness of chamber inside walls (1 mm). B) Varied number of chambers with a constant height of chambers (7 mm) and wall thickness (1 mm). C) Varied thickness of inside walls with constant height of chambers (10.5 mm) and number of chambers (5).

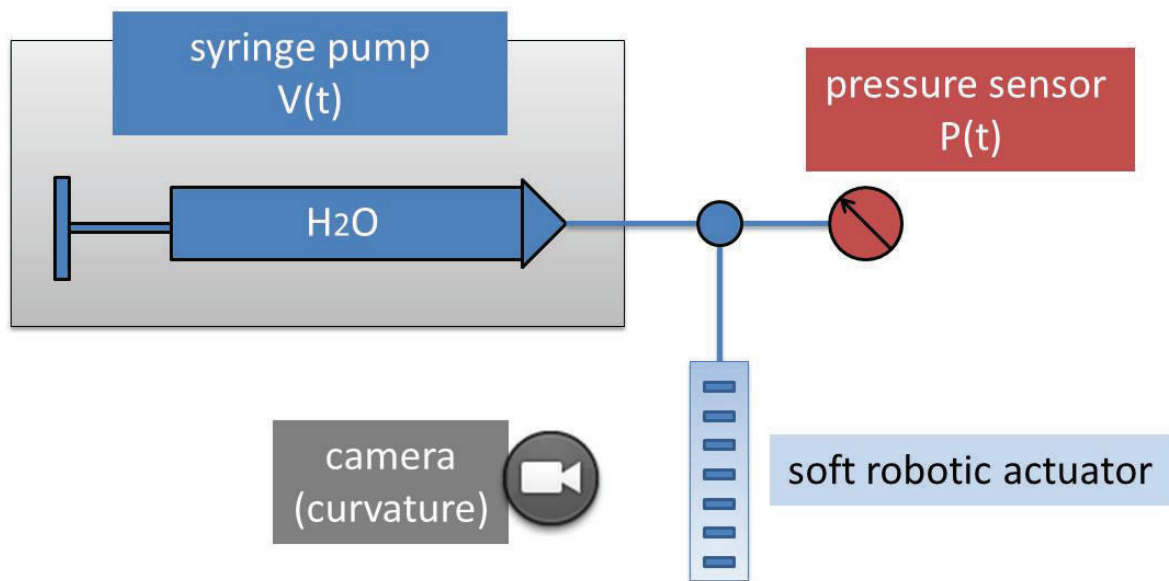


Figure S3. Experimental System to Measure Pressure-Volume Hysteresis Curves. A

programmable syringe pump infuses water to a T junction that was connected to a pressure sensor and the soft robotic actuator. Due to the incompressibility of water, the rate of infusion of the syringe pump was directly related to the changes in volume of the pneumatic channels of the actuator. Rates of infusion were chosen to be sufficiently low to achieve quasistatic conditions. To minimize the effect of gravity, the actuator was suspended in water within a fish tank made of glass. Bending of the actuator was monitored by a webcam.

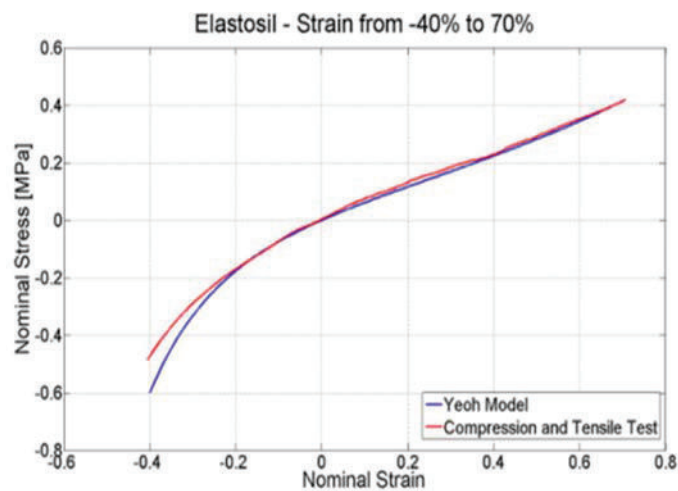


Figure S4. Stress-Strain Curve of Elastosil M4601. Compression and tensile tests of the elastomeric material (Elastosil M4601) used for simulations of the actuators. The stress-strain curve is fitted with the Yeoh model of hyperelasticity.

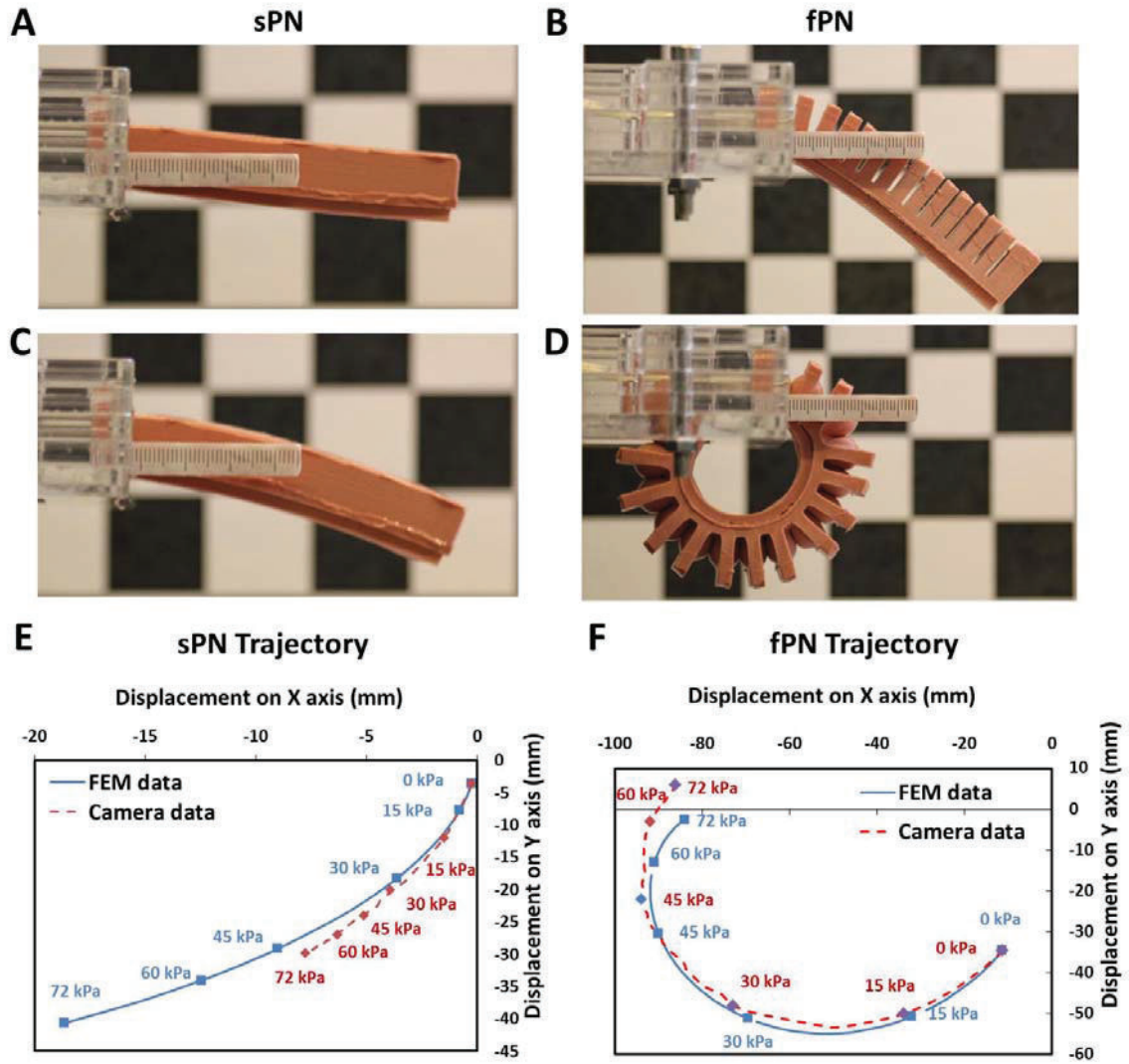


Figure S5. Bending of sPN and fPN actuator. A-D) Images of sPN (A,C) and fPN (B,D) actuators when pressurized with 0 kPa (0 psi) (A,B) and 72 kPa (10.44 psi) (B,D). Marks on the scale bar represent mm. E-F) Plot of trajectories for experimental and FEM tests for the tip of the free end of the sPN and fPN actuators at various pressures.

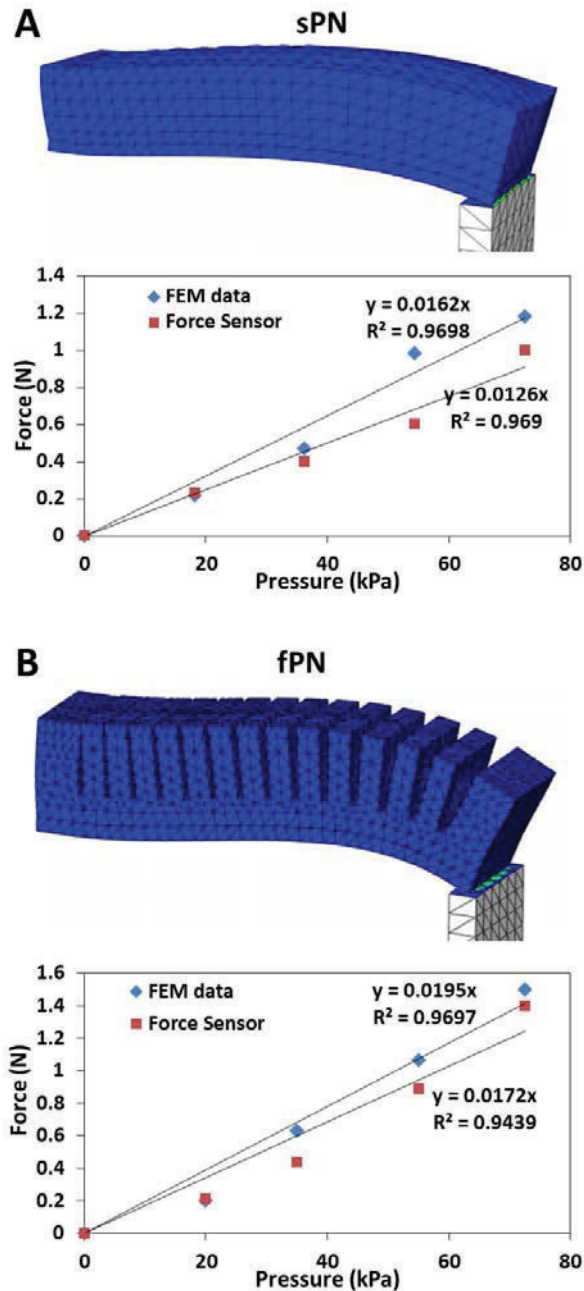


Figure S6. Force Exerted at Tip of Pneu-net. A-B) FEM model of a sPN (A), and fPN (B) to simulate the force exerted at its tip for several pressures. Plot includes data from both simulated and experimental measurements.

References:

- [1] F. Ilievski, A. D. Mazzeo, R. F. Shepherd, X. Chen and G. M. Whitesides, *Angew. Chem. Int. Ed.*, **2011**, 50, 1890.
- [2] R. F. Shepherd, F. Ilievski, W. Choi, S. A. Morin, A. A. Stokes, A. D. Mazzeo, X. Chen, M. Wang and G. M. Whitesides, *Proc. Natl. Acad. Sci. U.S.A.*, **2011**, 108, 20400.
- [3] R. F. Shepherd, A. A. Stokes, J. Freake, J. Barber, P. W. Snyder, A. D. Mazzeo, L. Cademartiri, S. A. Morin and G. M. Whitesides, *Angew. Chem. Int. Ed.*, **2013**, 52, 2892.
- [4] W. Gu, H. Chen, Y.-C. Tung, J.-C. Meiners, S. Takayama, *Appl. Phys. Lett.* **2007**, 90, 033505.
- [5] O. H. Yeoh, *Rubb. Chem. Tech.*, **1993**, 66, 754.